Intermetallics 31 (2012) 325–329

Contents lists available at SciVerse ScienceDirect

Intermetallics

journal homepage: www.elsevier.com/locate/intermet

Short communication

Saffman–Taylor fingering in nanosecond pulse laser ablating bulk metallic glass in water

Y. Liu [a], M.Q. Jiang [a,*], G.W. Yang [b], J.H. Chen [a], Y.J. Guan [a], L.H. Dai [a,*]

[a] State Key Laboratory of Nonlinear Mechanics, Institute of Mechanics, Chinese Academy of Sciences, No. 15, Beixihuanxi Road, Beijing 100190, China
[b] State Key Laboratory of Optoelectronic Materials and Technologies, School of Physics and Engineering, Zhongshan University, Guangzhou, Guangdong 510275, China

ARTICLE INFO

Article history:
Received 18 April 2012
Received in revised form
17 June 2012
Accepted 20 July 2012
Available online 30 August 2012

Keywords:
A. Intermetallics, miscellaneous
B. Surface properties
C. Laser processing
C. Rapid solidification processing

ABSTRACT

We report for the first time the nanosecond pulse laser ablation of a typical Zr-based (Vit 1) bulk metallic glass in a water environment, paying attention to the target surface morphology after ablation. Quite interestingly, a Saffman–Taylor fingering instability can be observed, which results from the strong interaction between the phase explosion-induced plasma plume and the resultant molten Vit 1 layer confined in the water medium. The instability condition is obtained via a perturbation analysis, and its characteristic size is well predicted. Our observations reveal the nature of liquid structure of metallic glasses.

1. Introduction

Laser ablation of solid targets in an atmosphere of liquids (mainly, water) is an intriguing technique for (i) producing micro/nano particles [1,2] that are very useful in material science, analytical chemistry and bioanalysis fields [3,4], (ii) material processing [5], (iii) surface modification of materials [6,7], and so on [8]. Promotion of these applications depends, to a large extend, on the in-depth understanding of the ablation mechanism, i.e., how material is liberated from the targets. Over the past decades, various methods have been developed to identify ablation mechanisms [9–14], among which target surface morphologies after ablation provide useful clues [5,6,15–17]. Bulk metallic glasses (BMGs) represent a relatively young class of materials with both glassy-state structure and metallic-bonding character, processing a series of superior properties [18–23] and showing widespread potential applications as structural and functional materials [24–28]. Due to rapid heating and cooling, lasers have been widely used to welding, cutting, cladding, alloying, glazing, annealing, melting or ablating the small-scaled amorphous alloys such as ribbons, films and wires [29–33], very recently extending to BMGs [34–37]. Through laser-processing, microstructures [29,31–33,37], magnetic properties [30], forming ability [38], and mechanical properties [35–37] of this kind of glassy alloys can be significantly improved, whereas only few works have focused on the surface patterns [39–41]. Furthermore, it is noted that, however, the laser-BMG interaction in a liquid-confined environment has not been reported yet. In this paper, for the first time, we performed nanosecond pulse laser ablations of a typical Zr-based BMG in a water medium. An interesting ablation surface morphology, viscous fingering, was observed, and its underlying mechanism was quantitatively discussed as well.

2. Experimental

We choose a typical $Zr_{41.2}Ti_{13.8}Cu_{12.5}NiB_{10}e_{22.5}$ (Vit 1) BMG as target materials: plates with the thickness of about 2 mm, the length of 10 mm and the width of 10 mm. The Vit 1 target was polished mirror-like, as shown in Fig. 1. The glassy structure of the targets was ascertained by X-ray diffraction (XRD) in a Philips PW 1050 diffractometer using CuKα radiation. It can be seen from Fig. 2 that the target before the laser ablation showed only broad diffraction maxima and no peaks of crystalline phases were visible. Fig. 3 shows a schematic diagram for the laser ablation to the Vit 1 BMG target. A Q-switched Nd:YAG solid state laser was used to generate the laser beam with wavelength of 532 nm, pulse width t_p of 10 ns, and maximum pulse energy of 500 mJ. The energy of laser pulse was measured by a joule meter (Coherent EPM 1000) prior to the practical ablations. The laser beam produced a Gaussian spatial

* Corresponding authors. Tel.: +86 10 82543958; fax: +86 10 82543977.
E-mail addresses: mqjiang@imech.ac.cn (M.Q. Jiang), lhdai@lnm.imech.ac.cn (L.H. Dai).

0966-9795/$ – see front matter © 2012 Elsevier Ltd. All rights reserved.
http://dx.doi.org/10.1016/j.intermet.2012.07.014

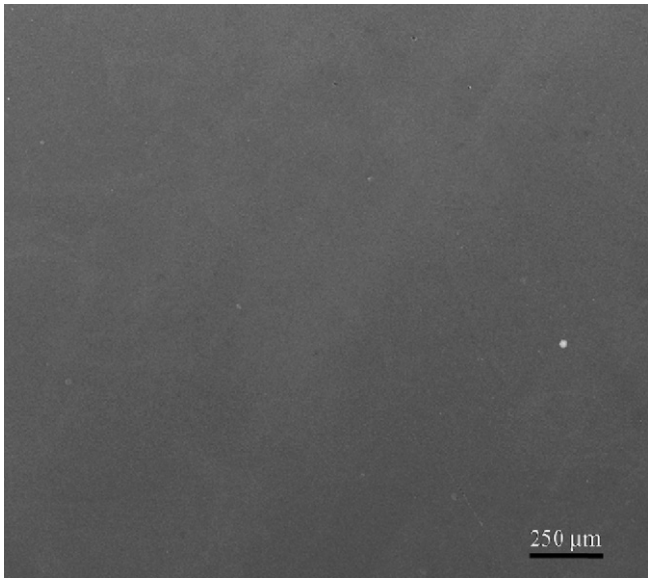

Fig. 1. SEM image of the Vit 1 target surface before the pulse laser ablation.

distribution of energy, and was focused by a lens at the surface of Vit1 BMG target. The target and was placed in a small beaker and a precise positioner was used to support the beaker for adjusting the target for the best focusing of the laser beam at the target surface. The environment water is filtered, de-ionized; the target was covered by 5 mm thick water layer, and then single pulse laser ablation experiments were performed. During the laser ablation, the target and water were maintained at room temperature and ambient pressure. Here, the pulse laser energy is fixed to be 300 mJ; thus the fluence is estimated to be about 238 J/cm^2 based on the observed ablated area with the diameter of about 400 μm [see Fig. 4(a)]. After ablation, a high-resolution scanning electron microscope (HRSEM, FEI Sirion, spatial resolution 1.5 nm) was used to examine the surface morphology of all targets. It is noted that there are no obvious phase change of ablation surface [see Fig. 2] due to the rapid heating and cooling rate during the pulse laser ablation.

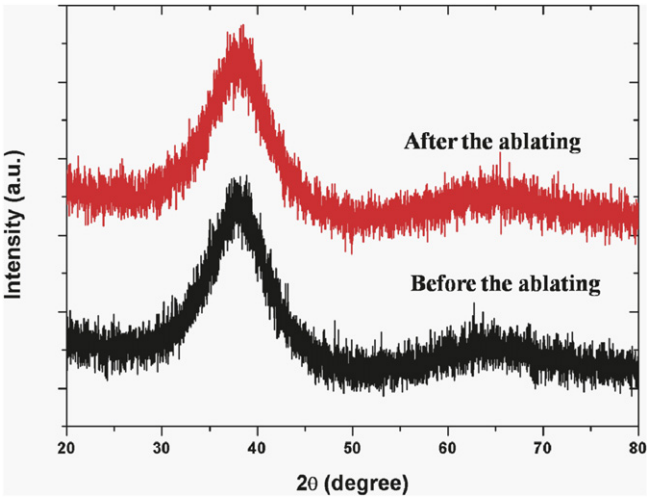

Fig. 2. XRD patterns for the ablation surface of the Vit 1 BMG before and after the pulse laser ablation.

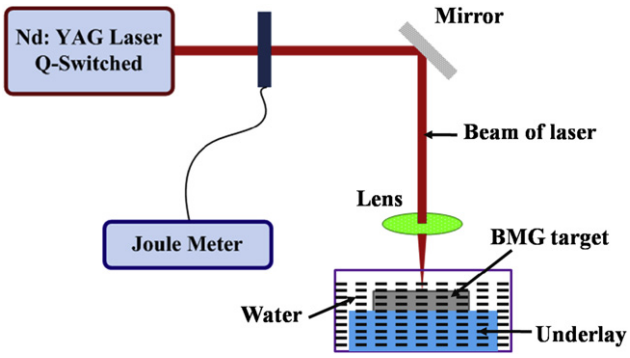

Fig. 3. Schematic for the pulse laser ablation to the Vit 1 BMG target.

3. Results and discussion

Fig. 4(a) presents the full-view of the typical surface morphology of the Vit 1 BMG target after the ablation. A high-magnification micrograph of the region "B" in Fig. 4(a) is shown in Fig. 4(b). It can be seen that the whole ablation area mainly consists of a relatively smooth central region "I" and a rough outer region "II" with the starfish-shaped boundary. Note that many ripples form near the edge of the ablated area and their characteristic spacing is about 1 μm, as shown in Fig. 4(c). The rough region "II" shows the cell-like vein patterns [see Fig. 4(d)], very similar to the fracture surface of this material under uniaxial compression [42]. It must be pointed out that, with the attendant cell-like patterns, many melted droplets and pores can be clearly observed. This implies that a significant thermomechanical process, i.e., material ejection, should occur in this region. A close-up view of the area "E" in Fig. 4(a) is presented in Fig. 4(e) and (f) at different magnifications. Surprisingly, the "arms of the starfish" are actually an interesting fingering phenomenon. The characteristic size of the fingers is of several micrometers.

The ablation morphology presented in Fig. 4 provides some paramount information that allows us to reveal the complex process of laser–BMG interaction in water. As compared with the case in ambient air [41], we find that the ablation in the present water case is much more aggravated. This means that the water plasma breakdown is not at work even in the current high-fluence case. If that happens, the amount of laser energy delivered to the target should remarkably decrease and the ablation of the target should be mitigated due to the strong absorption of the laser by the breakdown plasma in the environment water [7,16]. Therefore, the 532 nm laser light is absorbed mainly by the Vit 1 target via the transparent water. For one pulse duration, the thermal diffusion length $\sqrt{2\varsigma t_p} \sim 400$ nm that is large compared to the penetration depth $\alpha^{-1} \sim 10$ nm of the light [43], where ς is the heat diffusivity, 8.3×10^{-6} m^2/s for the Vit 1 BMG [44]. In this case, the temperature in the Vit 1 target heated by the laser beam satisfies that [45]:

$$T(z,t) = T_0 + 2\frac{(1-R)I_L}{\rho C}\sqrt{\frac{t}{\kappa}}\mathrm{ierfc}\left(\frac{z}{2\sqrt{\kappa t}}\right), \quad (1)$$

where ierfc is the inverse of the complementary error function, and z is the coordinate parallel to the laser beam. In this equation, the initial temperature T_0 is about 300 K, the optical reflectivity R is adopted as 0.4 [46], the incident light intensity I_L is 2.38×10^{14} W/m^2, the density ρ and the specific heat for Vit 1 BMGs are 6125 kg/m^3 and 400 J kg^{-1} K^{-1}, respectively [44,47].

Fig. 5 shows the estimated temperature with respect on time at 100 nm below surface based on Eq. (1). One can see that in a period of nanoseconds the temperature rises up to $\sim 10^5$ K. The extremely

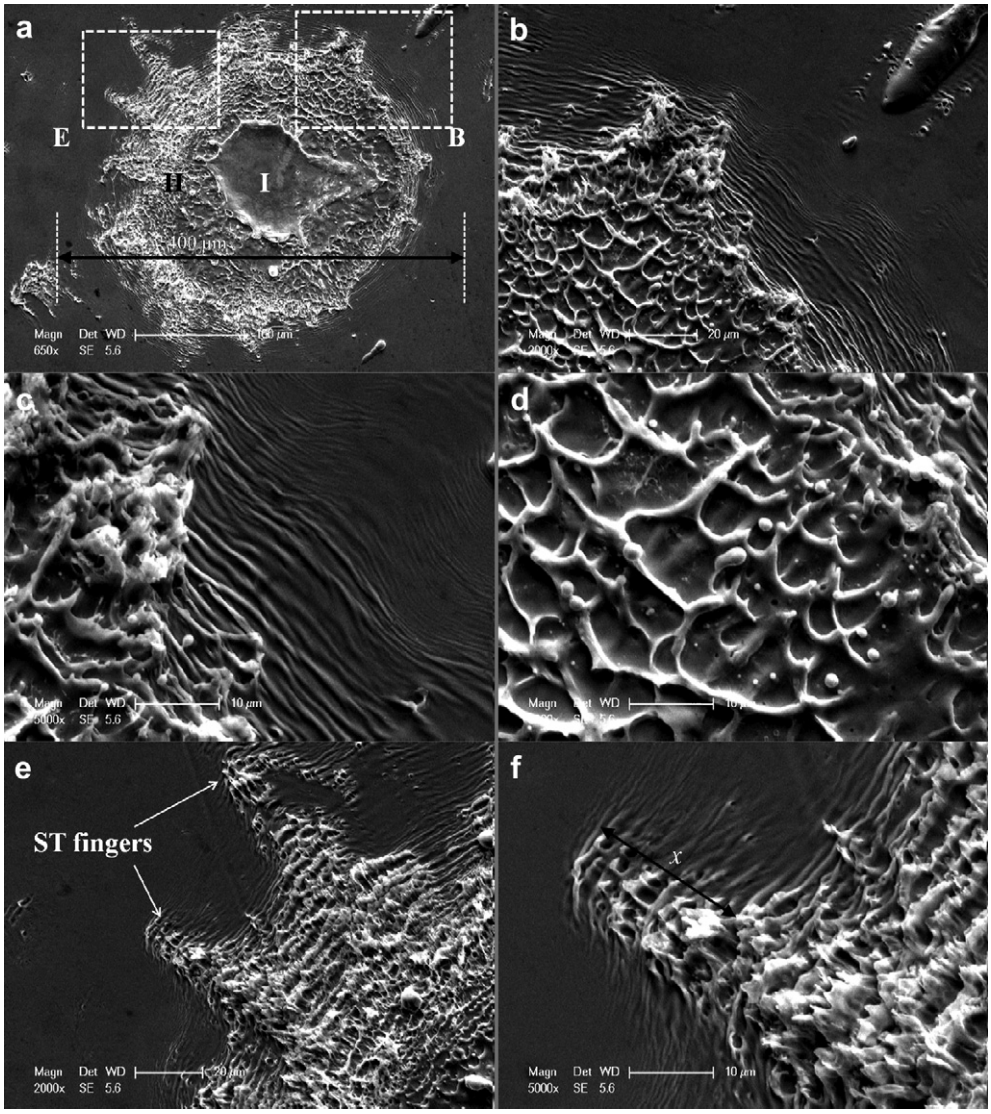

Fig. 4. The surface morphology of the Vit 1 BMG ablated by a nanosecond pulse laser with singe shot in a water environment. (a) The full view of ablated area consisting of a smooth region "I" and a rough region "II". (b), (c) and (d) Close-up views of the area "B" marked in (a) at different magnification. (e) and (f) correspond to the area "E" in (a), showing Saffman–Taylor fingering.

high temperature in such a thin Vit 1 layer excites a plasma at the Vit 1–water interface. The plasma then equilibrates with the surrounding water and Vit 1, leaving behind a molten Vit 1 layer on the surface. In the process, some of the water vaporizes or dissociates, generating an assembly of bubbles at the center of ablation area. This leads to a rounded smooth region "I", as shown in Fig. 4(a). According to the result shown in Fig. 5, one can estimate that the temperature rise rate at the irradiated surface is much greater than that necessary for phase explosion to occur, 10^9 K/s. This suggests that the molten layer in an atmosphere of the expanding plume further undergoes phase explosion and becomes less viscous, leaving behind the liquid droplets and pores at the ablated surface [see region "II" in Fig. 4]. The phase explosion, in turn, makes the plume expansion more intensive. It is expected that the expanding plume with low viscosity would penetrate into the more viscous molten-layer (i.e., the rippling region) outside the plume. The interface between them is liable to unstable; such configuration obeys the Saffman–Taylor (S–T) instability. Subsequently, it is interesting to seek the instability condition and predict the characteristic size of resultant patterns.

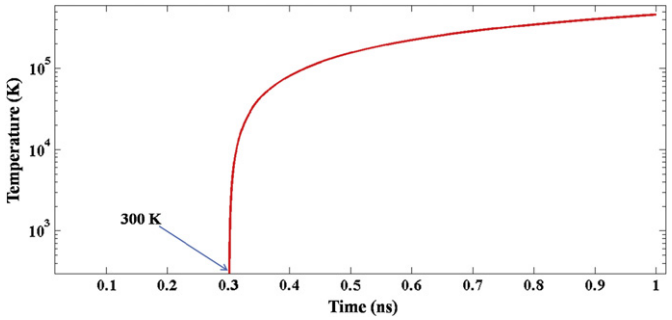

Fig. 5. Estimated time dependence of temperature at 100 nm below the target surface of Vit 1 BMG.

We consider the case where a less viscous plume pushes a more viscous Vit 1 melt, molded in an Eulerian coordinate system (x, y, z), as shown in Fig. 6. The incident direction of laser is along the negative z-axis; the plane (x, y) is the target surface. The

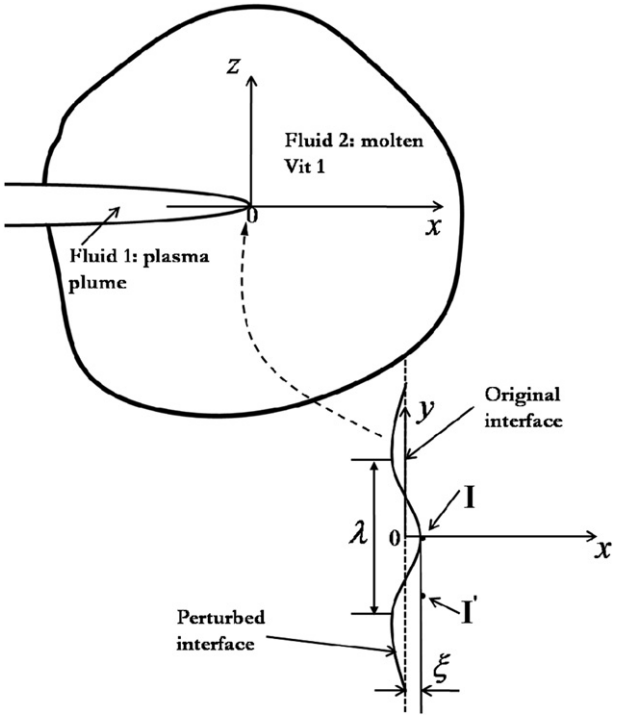

Fig. 6. Development of Saffman–Taylor fingering instability at a meniscus-shaped interface between the plasma plume and the molten Vit 1.

motion of both fluids is confined to a narrow gap between the water and the unmelted Vit 1. The fluid fields of both plume and Vit 1 melt satisfy the Navier–Stokes equation; their solutions are difficult to obtain due to the complicated boundary conditions. It is noted that we are only interested with the onset condition under which the interface between the two fluids will grow unstably to S–T fingering. Assume that the original plasma plume has a meniscus-shaped front with a local curvature κ that is determined by the surface tension σ and the negative pressure p at the point 0 by $\kappa = p/\sigma$. It must be pointed that the change of p along the x direction will advance the meniscus-shaped interface. Then the fluid meniscus is applied with a perturbation that is considered as an infinitesimal waviness in the y direction having a wavelength λ and an amplitude ξ in the x direction, as shown in the inset of Fig. 6. Now we focus on whether the perturbation will grow or die out by examining the transfer of flow between peaks and valleys of the waviness.

Due to the applied perturbation, the meniscus at point I requires a new negative principal curvature which produces a decrease in negative pressure at the interface to a level

$$p_{\mathrm{I}} = \sigma\left(\kappa + k^2\xi\right), \tag{2}$$

where $k = 2\pi/\lambda$ is a wave number. At position I′ in the melt at the same distance ξ as that of point I, the negative pressure is the same as that in its unperturbed state, i.e.

$$p_{\mathrm{I}'} = \sigma\kappa + \frac{\mathrm{d}p}{\mathrm{d}x}\xi. \tag{3}$$

where $\mathrm{d}p/\mathrm{d}x$ is the negative pressure gradient that drives the instability. If the negative pressure at I′ is larger than that at the new perturbed interface at I, the melt will flow from I to I′. In this case, the perturbation of that wavelength will grow into an S–T fingering, and the instability condition is

$$\frac{\mathrm{d}p}{\mathrm{d}x} \geq k^2\sigma. \tag{4}$$

This equation tells immediately a critical wavelength that may lead to runaway instability, i.e.

$$\lambda_{\mathrm{c}} = 2\pi\sqrt{\frac{\sigma}{\mathrm{d}p/\mathrm{d}x}}. \tag{5}$$

Perturbation with a wavelength smaller than λ_{c} will die out, whereas the one with a wavelength larger than λ_{c} will grow into S–T fingering. However, the instability usually occurs at a special set of wavelength or wave number, which is the dominant (fastest) mode instability. This dominant wavelength λ_{m} is usually $\sqrt{3}$ times λ_{c} [48,49]. In fact, λ_{m} corresponds to the width of the fingering observed finally. For the current nanosecond pulse laser on Vit 1 BMGs in water, the surface tension σ is 0.83 N m^{-1} [41], the surface pressure pulse is estimated to be about 20 atm [50]. Base on the Fig. 4(e) and (f), $x \sim 10$–20 μm, then we obtain that $\mathrm{d}p/\mathrm{d}x \sim 2$ atm/μm. Therefore, λ_{s} is calculated to be about several micrometers, in a good agreement with the experimental observations. Furthermore, the viscosity is a very important factor for the Vit 1 melts that should influence the S–T instability and resultant fingering morphology. For metallic glass melts, with increasing the viscosity, the surface tension usually increases, whereas the negative pressure gradient reduces. This leads to the increase of the critical wavelength for the instability [see Eq. (5)], implying the retardance of the S–T instability. On the other hand, if the S–T fingering instability can occur for the higher viscosity case, the final characteristic size of fingers should be larger than that for the lower viscosity case.

4. Conclusions

In summary, single pulse ablations of a Vit 1 BMG were performed by nanosecond lasers in a water-confined environment. The target surface morphology after the ablation provides clearer evidence for the phase explosion mechanism in present ablation case. The phase explosion results in ejection of material in the form of a plume, which acts on the molten Vit 1 layer due to the confinement of water. Such interplay between them produces an interesting hydrodynamic instability phenomenon, i.e., Saffman–Taylor fingering. The experimental observations may lend new insight into the mechanism for the pulse laser ablation of BMGs in liquids and even the nature of liquid structure of metallic glasses.

Acknowledgments

Financial support is from the NSFC (Grants Nos. 11132011, 11002144, 11021262 and 11023001), the National Natural Science Foundation of China-NSAF. Grant No: 10976100 and the National Key Basic Research Program of China (Grant No. 2009CB724401 and 2012CB937500).

References

[1] Phuoc TX, Howard BH, Martello DV, Soong Y, Chyu MK. Opt Laser Eng 2008; 46:829.
[2] Nichols WT, Sasaki T, Koshizaki N. J Appl Phys 2006;100:114912.
[3] Henglein A. J Phys Chem 1993;97:5457.
[4] Meunier M, Sylvestre JP, Kabashin AV, Sacher E, Luong JHT. J Am Chem Soc 2004;126:7176.
[5] Morita N, Ishida S, Fujimori Y, Ishikawa K. Appl Phys Lett 1988;52:1965.
[6] Shen MY, Crouch CH, Carey JE, Mazur E. Appl Phys Lett 2004;85:5694.
[7] Wu BX, Shin YC. J Appl Phys 2007;101:103514.
[8] Compagnini GC, Mita V, Catallotti RS, D'Urso L, Puglisi O. Carbon 2007;45: 2456.

[9] Kelly R. In: Chrisey DB, Hubler GK, editors. Pulsed laser deposition of thin films. New York: Wiley; 1994.
[10] Zhu S, Lu YF, Hong MH. Appl Phys Lett 2001;79:1396.
[11] Sakka T, Saito K, Ogata YH. J Appl Phys 2005;97:014902.
[12] Evans R, Camacho-Lopez S. J Appl Phys 2010;108:103106.
[13] Wu BX. Appl Phys Lett 2008;93:101104.
[14] Kim BM, Komashko AM, Rubenchik AM, Feit MD, Reidt S, Da Silva LB, et al. J Appl Phys 2003;94:709.
[15] Choo KL, Ogawa Y, Kanbargi G, Otra V, Raff LM, Komanduri R. Mater Sci Eng A 2004;372:145.
[16] Nichols WT, Sasaki T, Koshizaki N. J Appl Phys 2006;100:114911.
[17] Chen XY, Lin J, Liu JM, Liu ZG. Appl Phys A 2009;94:649.
[18] Greer AL. Science 1995;267:1947.
[19] Johnson WL. MRS Bull 1999;24:42.
[20] Inoue A. Acta Mater 2000;48:297.
[21] Löffler JF. Intermetallics 2003;11:529.
[22] Wu Y, Li HX, Chen GL, Hui XD, Wang BY, Lu ZP. Scripta Mater 2009;61:564.
[23] Wang WH. Prog Mater Sci 2012;57:487.
[24] Conner RD, Dandliker RB, Scruggs V, Johnson WL. Int J Impact Eng 2000;24:435.
[25] Grimberg A, Baur H, Bochsler P, Bühler F, Burnett DS, Hays CC, et al. Science 2006;314:1133.
[26] Wu Y, Xiao YH, Chen GL, Liu CT, Lu ZP. Adv Mater 2010;22:2770.
[27] Huang X, Ling Z, Liu ZD, Zhang HS, Dai LH. Int J Impact Eng 2012;42:1.
[28] Axinte E. Mater Des 2012;35:518.
[29] LaGrange T, Grummon DS, Reed BW, Browning ND, King WE, Campbell GH. Appl Phys Lett 2009;94:184101.
[30] Sorescu M. Phys Rev B 2000;61:14338.
[31] Radlinski AP, Calka A, Lutherdavies B. Phys Rev Lett 1986;57:3081.
[32] Sun H, Flores KM. Metall Mater Trans A 2010;41A:1752.
[33] Sun H, Flores KM. J Mater Res 2008;23:2692.
[34] Kawahito Y, Terajima T, Kimura H, Kuroda T, Nakata K, Katayama S, et al. Mater Sci Eng B 2008;148:105.
[35] Matthews DTA, Ocelik V, de Hosson JTM. Mater Sci Eng A 2007;471:155.
[36] Chen BQ, Pang SJ, Han PP, Li R, Yavari AR, Vaughan G, et al. J Alloys Compd 2010;504:S45.
[37] Wu G, Li R, Liu Z, Chen B, Li Y, Cai Y, et al. Intermetallics 2012;24:50.
[38] Audebert F, Colaco R, Vilar R, Sirkin H. Scripta Mater 2003;48:281.
[39] Liu KX, Liu WD, Ye LM. J Appl Phys 2011;109:043109.
[40] Ma FX, Yang JJ, Zhu XN, Liang CY, Wang HS. Appl Surf Sci 2010;256:3653.
[41] Liu Y, Jiang MQ, Yang GW, Guan YJ, Dai LH. Appl Phys Lett 2011;99:191902.
[42] Jiang MQ, Ling Z, Meng JX, Dai LH. Philos Mag 2008;88:407.
[43] Jiang MQ, Duan GH, Dai LH. J Non-Cryst Solids 2011;357:1621.
[44] Jiang MQ, Dai LH. J Mech Phys Solids 2009;57:1267.
[45] von Allmen M, Luthy W, Siregar MT, Affolter K, Nicolet MA. Annealing of silicon with 1.06 μm laser pulses. In: Ferris SD, Leamy HJ, Poate JM, editors. Laser–solid interactions and laser processing-1978. Boston: American Institute of Physics; 1979. p. 43.
[46] Lapka R, Leemann G, Guntherodt HJ. Mater Sci Eng A 1988;99:313.
[47] Bai HY, Luo JL, Chen ZJ, Wang WH. Appl Phys Lett 2001;78:2697.
[48] Argon AS, Salama MS. Mater Sic Eng 1976;23:219.
[49] Spaepen F. Acta Metall 1975;23:612.
[50] Bennett TD, Grigoropoulos CP, Krajnovich DJ. J Appl Phys 1995;77:849.